
Proceedings of Ninth World Conference on Earthquake Engineering
August 2-9, 1988, Tokyo-Kyoto, JAPAN (Vol.IV)

6-3-13

AN ANALYTICAL STUDY OF SEISMIC RESISTANT ECCENTRICALLY BRACED STEEL FRAMES

James M. RICLES[1] and Egor P. POPOV[2]

[1]Assistant Professor of Structural Engineering,
Department of Applied Mechanics and Engineering Science,
University of California at San Diego, La Jolla, California, USA
[2]Professor Emeritus of Civil Engineering,
University of California at Berkeley, Berkeley, California, USA

SUMMARY

Presented are results of an analytical study of seismic resistant eccentrically braced frames, EBFs, subjected to severe earthquakes. The purpose of this study was to assess current EBF seismic design criteria involving short links designed to yield in shear. Two EBFs were designed and analyzed for response to different earthquake accelerograms using inelastic time history procedures. Parameters which were investigated included the effects of strain hardening and composite action. In order to assure accurate results, link and composite beam-column elements were developed based on experimental data to model floor beams in EBFs.

INTRODUCTION

An EBF is a braced frame in which the braces are offset from adjacent braces, thereby creating an eccentricity in the floor beams. For some EBF configurations the eccentricity in the floor beams is created by offsetting the braces from columns. The part of a floor beam which defines the eccentricity is referred to as a link. The design of an EBF is based on the principle that during overloading the links yield and act as ductile members, thereby inhibiting brace and column buckling, for these member forces are therefore limited by the ultimate forces developed in the links. The members outside the links are designed to resist the ultimate capacity of the link in an elastic manner, thereby assuring a ductile structural system. This form of design is known as capacity design. Current design criteria for short links bases the ultimate link strength on a shear force of $1.5V_p$, where $V_p = 0.55\ F_y dt_w$ and is the plastic shear strength of the steel floor beam. Link deformation is limited in order to prevent link failure due to excessive web buckling which may lead to link web tearing and strength deterioration. The above criteria are based on test data obtained using EBF subassemblies under pseudo-static cyclic loading conditions. To assess these provisions for more realistic conditions, inelastic dynamic time history analysis of EBFs were performed (Ref. 1). Specially developed elements were used to model the links and composite floor beams outside the links for random cyclic loading.

Link Element Formulation The link element was based on a stress resultant formulation and consisted of an elastic beam with rigid-plastic hinges at each end (Ref. 1), as shown in Fig. 1(a). The EBFs were analyzed as planar frames, therefore only the effect of in plane forces had to be considered in the link

element. Each hinge consisted of a set of three subhinges of zero length, see Fig. 1(b), with each subhinge having a yield surface in moment-shear force space. The yield surfaces were concentric in order that the three subhinges of a hinge would sequentially yield at specific force levels. The behavior of the combined elastic beam element and two hinges consisted of elastic shear, flexural and axial deformations developing in the elastic beam, with inelastic shear and flexural deformations developing in yielded subhinges. This produced a force-deformation response consisting of an initial elastic curve followed by a reduction in stiffness in three steps under increased load which resulted in sequential yielding of all subhinges. A tangent stiffness matrix, $\underline{K}_T$, was calculated for the element by forming the tangent flexibility matrix, $\underline{F}_T$, and then equating $\underline{K}_T$ to the inverse of $\underline{F}_T$. $\underline{F}_T$ is equal to the combined flexibility of the elastic beam, $\underline{F}$, and yielded subhinges $\underline{f}_p$: Since each subhinge had rigid-plastic behavior only yielded subhinges contribute to $\underline{f}_p$. The forces resulting in element deformations θ_i, θ_j, and γ are the moments at the element's ends, M_i and M_j, and shear V, where θ_i and θ_j are flexural deformations at end i and j, respectively, and γ shear deformation. Based on experimental data (Ref. 2), a series of rectangular yield surfaces was selected for each subhinge. Experimental data also indicated that both isotropic and kinematic hardening occurred in links yielding predominantly in shear. Therefore, an anisotropic hardening rule was devised for each subhinge where isotropic and kinematic hardening occurred in shear, with moment yielding following only a kinematic hardening rule.

Composite Beam-Column Element Formulation To effectively model the floor beam in a braced EBF bay outside the link, the change in stiffness of this member under moment reversal observed during experiments (Ref. 2) had to be accounted for. Although these experiments on EBFs with composite floors indicated that the floor beam outside the link remained elastic, an element was developed which allowed for yielding considering axial load-moment interaction (Ref. 1). A typical cyclic force-deformation curve for moment causing load reversal and yielding for the element is shown in Fig. 2. The element was based on in plane forces and consisted of the well known parallel component beam-column model in series with a zero length rigid-plastic rotational hinge at each end, as shown in Fig. 2. The purpose of the hinges was to add flexibility to the parallel component model upon moment reversal in order to obtain the change in stiffness depicted in Fig. 2. Inelastic deformations resulting in a reduced stiffness due to yielding of the composite beam-column element were assumed to occur only in the parallel component model.

Both the link and composite beam-column elements were implemented into a computer program for the nonlinear static and dynamic analysis of structures (Ref. 1). Before analyzing EBFs for inelastic dynamic response, the elements' formulations were verified. This involved modeling several test specimens of bare and composite links in EBF subassemblies (Ref. 2) and a three story EBF, all of which were subjected to severe static cyclic loading. The response predicted by an analysis of a bare steel EBF subassembly consisting of a link and floor beam is shown in Fig. 3. The results show excellent agreement with the experimental data. Similar agreement was also achieved for the analysis of the other test specimens.

EBF ANALYSIS

EBF Design Using the capacity design concept described previously, and equivalent static lateral seismic loads per NEHRP (Ref.3), the two EBFs shown in Fig. 4 were designed, where both designs (Designs 1 and 2) had all moment connections. NEHRP provisions are based on ultimate loads with an inverted triangular distribution for the equivalent lateral loads. The EBFs, with all moment connections, were considered as dual systems. The links were designed as

short members where $e < 1.6M_p/V_p$, in which e and M_p are the link length and plastic moment capacity. The exterior columns adjacent to the links at the lower three floors were designed based on magnified moments, $M_{col}=\omega M_{code}$, where ω is an amplification factor applied to column moments M_{code} from an elastic static analysis to account for dynamic amplification and movement of the point of inflection in the columns during an extreme seismic event. A value of 1.8 for ω was used. The EBF designs were checked for compliance with the NEHRP code by means of elastic analysis. This included checking whether the total link deformation γ exceeded the maximum permissible value of ± 0.06 rad. The plastic deformations for determining the maximum γ were estimated by magnifying the elastic deformations by the factor $(C_d - 1)$, as suggested in the NEHRP code. C_d is equal to five for an EBF. Under the lateral loads, the link shears were restricted to be less than or equal to V_p in order to comply with the NEHRP provisions.

Program of Investigation The two EBF designs were subjected to the NS component of the 1940 El Centro earthquake record which had been scaled by a factor of 1.5, and the NE component of the 1966 Parkfield earthquake record. As a result, both of these records had a peak ground acceleration of 0.5g. These particular earthquakes were selected and scaled as noted in order to study the EBF response involving several significant cycles of yielding (1.5*El Centro) and large excursions of plastic deformation due to large pulses (Parkfield). The information to define the force-deformation relationships for the elements was based on experimental data (Ref.2). Design 1 was analyzed assuming bare steel behavior, both with and without strain hardening. Design 2 was analyzed assuming bare steel and composite behavior, respectively, with strain hardening. Both an interior and exterior composite EBF were considered. The composite links were modeled using the link element with a 5 and 17 percent greater initial shear yield strength, respectively, for the exterior and interior composite EBFs relative to the bare steel EBF model.

Results The envelopes of the story shear forces representing maximum and minimum values for Design 1 are shown in Fig. 5 for the response of EBF models with straining hardening to the Parkfield and scaled El Centro records. Included are results of EBF analysis assuming elastic-perfectly plastic behavior (EPP), as well as the design story shear forces per NEHRP. The effects of strain hardening are shown to be pronounced, where the base shears for the El Centro and Parkfield analysis were, respectively, 1.31 and 1.46 times greater than that of the corresponding EPP analysis. The response envelopes exceed the design envelope because larger beam sections with greater capacity were used in order to limit γ in the links per the elastic design check, and the fact that the design envelope does not include strain hardening. The corresponding maximum link shear forces, V_{max}, for each floor have been normalized by their respective values of V_p, and are plotted in Fig. 6. The analyses with strain hardening had all of the links in the bottom five floors yield, with the largest values of V_{max} developing in the first floor ($1.55V_p$) for both earthquakes. The Parkfield record caused more strain hardening in the upper floors than the scaled El Centro record, however for both analyses the first and second floor links developed a V_{max} equal to or greater than $1.5V_p$. The envelopes of maximum link deformation γ_{max} are shown in Fig. 7 where it is apparent that the lower floors developed larger values of γ_{max} than the upper floors. The Parkfield record caused larger link deformation, and resulted in γ_{max} exceeding the NEHRP design limit of 0.06 rad. in the lower three floors. The scaled El Centro record caused γ_{max} to exceed 0.06 rad. only in the first floor. Consideration should be given to increasing the bottom floor link sizes in order to reduce γ. The envelope of axial brace force for the analyses involving strain hardening are compared in Fig. 8 to the design envelop for compression based on $1.5V_p$ and to the EPP analysis. With strain hardening, greater axial brace forces developed, particularly in the lower floors where the Parkfield earthquake caused compressive axial brace forces in floors 1 and 2 to exceed the design envelope based on $1.5V_p$. The scaled El Centro record is shown

to have resulted in the first floor brace achieving an axial force equal to a value corresponding to a shear of $1.5V_p$ in the link. The effect of strain hardening resulted in a maximum increase of 41 and 29 percent, respectively, in the first floor bracing during the Parkfield and scaled El Centro earthquakes compared to the EPP analysis.

The columns in the EBFs were designed on the basis of all of the links simultaneously developing a shear force of $1.5V_p$. A comparison of the resulting design envelope for compressive axial column force with the response of the EBF models with strain hardening, shown in Fig. 9, indicates this to be a conservative assumption for the interior columns. The exterior columns show a much closer agreement with the design envelope, particularly the Parkfield earthquake where larger link shear forces developed in each of the bottom three floors. The significance of applying the amplification factor ω to the column moments M_{code} is demonstrated by the behavior of the bending moments in the exterior columns in Fig. 10, where it is shown at time t=5.0 sec. that the column moments above and below the first floor are not equal, as well as at the second floor. Furthermore, the point of inflection in the columns above the first three floors have shifted away from the column midheights. At time t=4.5 sec. these phenomena are also evident at the first floor. The above phenomena are a consequence of link yielding, where at t=4.5 sec. the first floor link was yielding, and at t=5.0 sec. all three bottom floor links were yielding. The columns of the bottom three floors would have yielded if it had not been for the application of the ω factor to the moments M_{code}.

The envelopes of story shear forces for Design 2 subjected to the Parkfield earthquake record are shown in Fig. 11, where results for analyses assuming bare steel and composite floor slab behavior are plotted. Composite action is shown to have increased the story shear forces, with the exterior composite EBF having a 3 percent increase in base shear and the interior composite EBF a 10 percent increase. Similar results were found for the response to the scaled El Centro earthquake. Envelopes of maximum link shear force, V_{max}, are compared in Fig. 12 for the Parkfield earthquake. In the lower four floors, composite action in the interior and exterior EBFs resulted in an increase of 10 and 4 percent in V_{max} relative to the bare steel EBF model. At the first floor the maximum shear force in the link of the bare steel EBF model was $1.5V_p$, while the interior and exterior composite EBFs, respectively, had values of 1.65 and $1.55V_p$. Similar results were found for the second and third floor links, with smaller increases occurring in the remaining upper floor links of the composite EBFs. The effect of larger link forces in the composite EBFs is evident in the axial brace force envelopes given in Fig. 13 for the bare steel and interior composite EBF, where the bottom four floors show an average of 12 percent increase in axial brace force relative to the bare steel EBF. The design envelope appears to be satisfactory in the upper floors for the bare steel results, although the first floor exceeded this envelope by 5 percent. The interior composite EBF exceeded the design envelope by an average of 11 percent in the lower three floors.

An examination of the inelastic action in Designs 1 and 2 indicated that only a minute amount of yielding occurred outside the links, where some of the floor beams in the unbraced bays and outside the links in braced bays yielded. The ductility demand placed on these members however was small. The links accounted for over 98 percent of the energy dissipated by the EBF models.

CONCLUSIONS

Based on the analytical investigation of the inelastic response of the 6 story, 3 bay EBF involving short links, the following conclusions are noted:
1) Capacity design can successfully be applied to EBFs in order to confine the inelastic action primarily to the links. To apply this concept, a designer

must know the ultimate link capacity. For short bare links in these analyses this capacity was found to be as large as $1.55V_p$ at the first floor. A maximum shear equal to $1.65V_p$ was found for the interior composite EBF. This phenomenon should be carefully considered when designing the braces and columns of EBFs with composite floors systems where significant link strain hardening is expected.

2) The column moments were found to be nonuniformly distributed above and below yielded links, resulting in the movement of the column's point of inflection. In view of this fact, great care must be taken when designing columns and column splices.
3) The assumption of all links simultaneously yielding for establishing column design axial forces was found to be satisfactory for the lower three floors. In the remaining upper three floors this assumption was more conservative.

REFERENCES

1) Ricles,J.M., and Popov,E.P.,"Dynamic Analysis of Seismically Resistant Eccentrically Braced Frames," Earthquake Engineering Research Center Report No. 87-07, Univ. of Calif., Berkeley, Calif. June 1987.
2) Ricles,J.M., and Popov,E.P.,"Experiments on Eccentrically Braced Frames with Composite Floors," Earthquake Engineering Research Center Report No. 87-06, Univ. of Calif., Berkeley, Calif. June 1987.
3) National Earthquake Hazards Reduction Program, Recommended Provisions for the Development of Seismic Regulations for New Buildings, Seismic Safety Council, Fed. Emergency Management Agency, Wash. D.C., 1985.

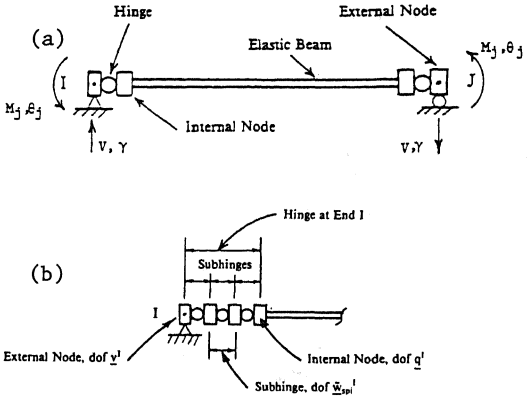

Fig.1 (a) Link element with (b) subhinges.

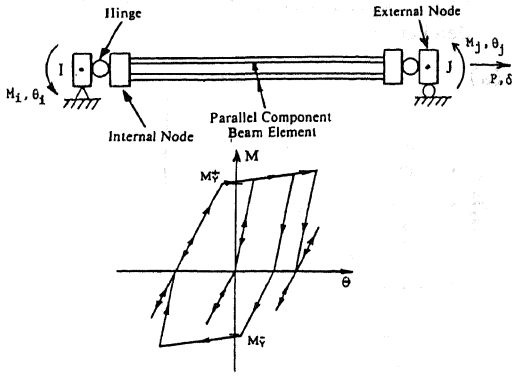

Fig.2 Composite beam-column element.

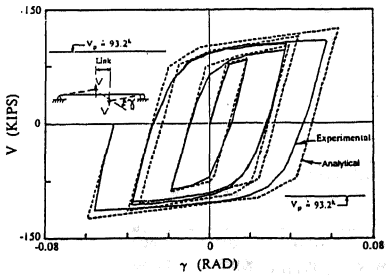

Fig.3 Analytical and experimental comparison.

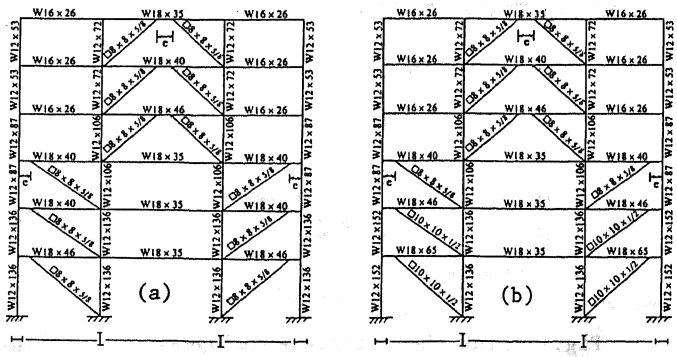

Fig.4 EBF (a) Design 1 and (b) Design for analysis

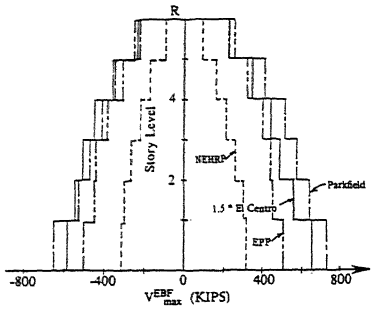

Fig.5 Story Shear envelopes for Design 1.

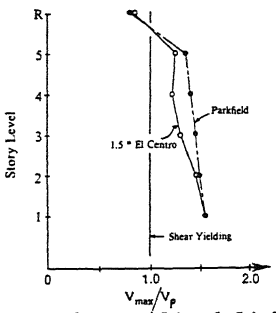

Fig.6 Normalized link shear envelopes, Design 1.

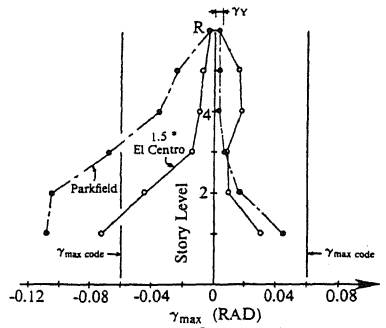

Fig.7 Link deformation envelopes, Design 1.

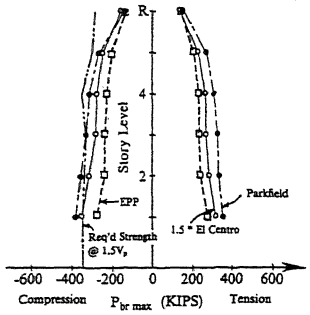

Fig.8 Axial brace force envelopes, Design 1.

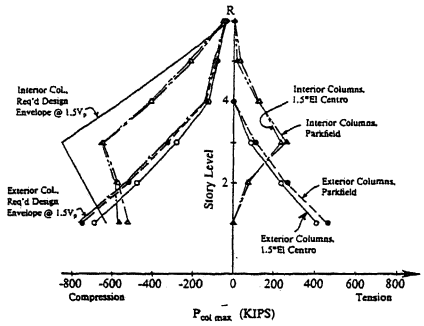

Fig.9 Axial column force envelopes, Design 1.

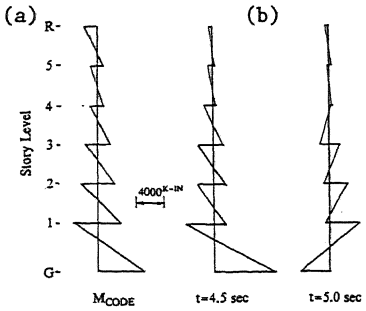

Fig.10 Exterior column (a) design moments with no amplification, and (b) moments at selected times, Design 1.

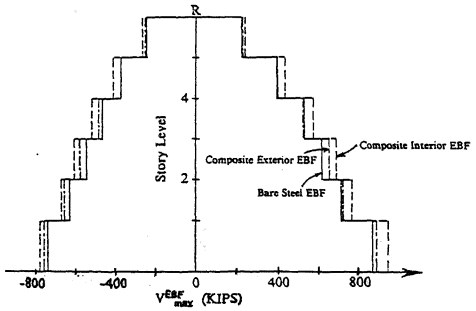

Fig.11 Story shear envelopes, Design 2.

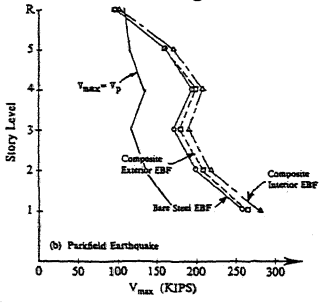

Fig.12 Link shear force envelopes, Design 2.

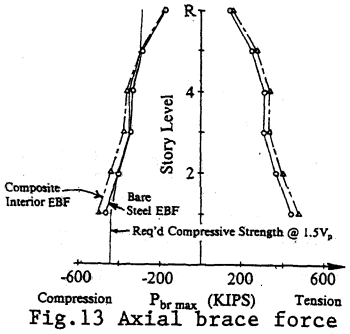

Fig.13 Axial brace force envelopes, Design 2.